Journal of Applied Mechanics and Technical Physics, Vol. 42, No. 4, pp. 659–664, 2001

NUMERICAL SIMULATION OF THE FALL OF A BODY WITH A CORRUGATED BOTTOM ON WATER

N. A. Taranukha and S. D. Chizhiumov

UDC 532.5:518.12:629.12.01.011.1

A numerical model is proposed for the potential flow of an ideal incompressible fluid produced by impact of a body with concave bottom on water. Compression of the entrapped air is taken into account. The algorithm is based on joint solution of the equations of motion for the body and the fluid by the finite difference method with approximation in time. At each time, the boundary-value problem for the Laplace equation is solved by the boundary-element method. Calculation results are given. The effects of the air layer, dimensions and shape of the corrugations, initial velocity, and other parameters on the impact process are shown.

Introduction. The motion of a vessel during waving involves possible baring of its head bottom followed by an impact on water (bottom slamming). The loads due to the impact are governed by the complex processes of rolling, fluid flow, and deformation of the bottom. When between the bottom and the water surface there is an air layer, whose characteristics are random quantities, simulation of slamming is considerably complicated.

In the present paper, we consider the possibility of decreasing impact pressures by replacing a flat ship bottom by concave or corrugated bottoms (Fig. 1). This shape of the bottom and the damping action of air lead to gradual submergence rather than a planar impact, and the fluid can be considered incompressible. At the initial time of submergence, the volume of the air layer is determined mainly by the shape of the corrugated bottom surface and, to a lesser degree, by the shape of random secondary waves on the water surface. As a result, the impact becomes less dependent on random factors. A corrugated shell has much higher stiffness than the plates of a flat bottom, and, hence its strains can be ignored in determining hydrodynamic loads.

The fluid flow is considered inviscid and irrotational. The air in the cavern is treated as an ideal gas, whose compression proceeds adiabatically. Strictly speaking, these assumptions are valid only for submergence at an early stage, which is of greatest interest because it is characterized by highest pressures. In the process of submergence, the pressure profile in the gas cavern becomes more nonuniform, eddies form in the fluid, phase changes occur, and damped pressure oscillations and other effects are observed. Neglect of these phenomena lowers the accuracy of the numerical model. However, for analysis of the initial stage of the process, the proposed model is fairly accurate for practice at low computational cost and can be used in multivariant calculations in design problems.

Numerical calculations of the submergence of bodies with a carinate bottom have been widely employed in experimental studies. Models of a viscous fluid are usually constructed by the finite difference method [1]. Potential flows of an ideal fluid are frequently analyzed by the finite element method [2–4]. At the same time, nonstationary flows with gas caverns have been studied inadequately [5].

In the present paper, the submergence process is simulated numerically using an algorithm based on a finite-difference approximation of the equations of motion with the parameters in each time step determined by the boundary-element method (BEM) [6]. The BEM allows one to determine flow characteristics only on the fluid boundary, thus reducing the number of nodes by an order of magnitude. In this case, the conditions at infinity are easily satisfied and the construction of the calculation grid is simplified as much as possible.

Komsomol'sk-on-Amur State Technical University, Komsomol'sk-on-Amur 681013. Translated from Prikladnaya Mekhanika i Tekhnicheskaya Fizika, Vol. 42, No. 4, pp. 112–118, July–August, 2001. Original article submitted January 9, 2001.

0021-8944/01/4204-0659 $25.00

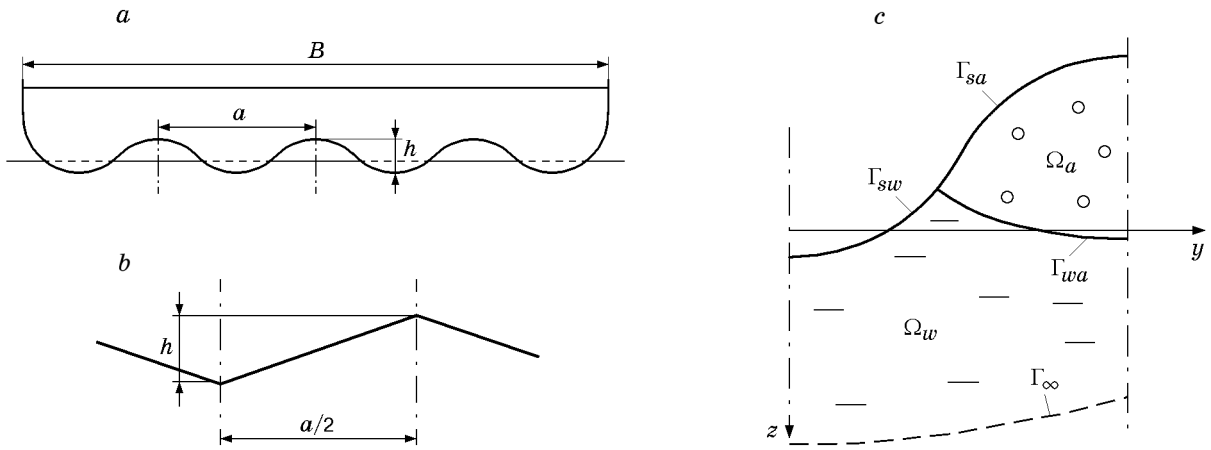

Fig. 1. Formulation of the problem: (a) corrugated surface; (b) triangular corrugation; (c) wavy corrugation.

Formulation of the Problem. At the moment the corrugated bottom touches the water surface, closed air caverns form (region Ω_a in Fig. 1). The aqueous medium (region Ω_w) is considered an ideal incompressible fluid, and the air in the cavern is treated as an ideal gas, whose compression proceeds adiabatically and is described by the Poisson equation

$$\frac{p_a(t_i)}{p_a(t_{i-1})} = \Big(\frac{V(t_{i-1})}{V(t_i)}\Big)^\gamma, \tag{1}$$

where p_a is the gas pressure, t_i is time, V is the volume of the cavern, and γ is the adiabatic exponent. Here and below, the quantities with the subscripts s, a, and w correspond to the body, the gas, and the fluid, respectively.

In the region Ω_w, the fluid motion is described by the Lagrange integral

$$\Big(\frac{\partial\varphi}{\partial t}\Big)_w + \frac{1}{2}\,v_w^2 + gz_w + \frac{p_w - p_0}{\rho_w} = 0, \tag{2}$$

where φ is the fluid velocity potential, v_w is the velocity, g is the free-fall acceleration, z_w is the z-coordinate reckoned from the free undisturbed fluid surface, p_w is the fluid pressure, p_0 is the atmospheric pressure, and ρ_w is the fluid density.

Equations (1) and (2) are related by the condition of pressure equality at the interface Γ_{wa}:

$$p_w = p_a. \tag{3}$$

In the case of free fall, the motion of the body is defined by the equation

$$M(g + \dot v_s) = \int\limits_{\Gamma_{sw}} (p_{sw} - p_0)\cos(\boldsymbol{n}, z)\,d\Gamma + \int\limits_{\Gamma_{sa}} p_a \cos(\boldsymbol{n}, z)\,d\Gamma, \tag{4}$$

where M is the mass of the body, p_{sw} is the pressure on the wetted surface of the body, and $\boldsymbol{n}$ is a normal to the surface.

At each time, the fluid velocity potential field is determined from the solution of the boundary-value problem for the Laplace equation:

— in the region Ω_w,

$$\Delta\varphi_w = 0; \tag{5}$$

— on the boundary Γ_{sw},

$$\frac{\partial\varphi_w}{\partial\boldsymbol{n}} = v\cos(v, \boldsymbol{n}); \tag{6}$$

— on the boundary Γ_{wa},

$$\varphi_w = \varphi_w^0; \tag{7}$$

— on the boundary Γ_∞,

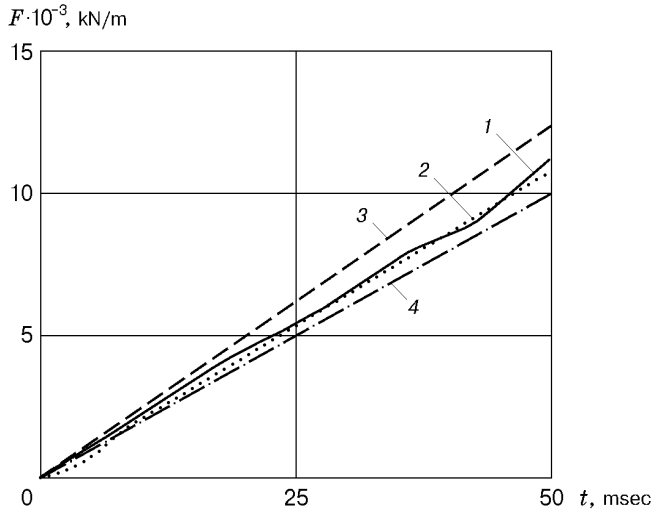

Fig. 2. Submergence force for a wedge versus time: curve 1 refers to calculations using the FEM [3], curve 2 refers to calculation using the BEM, and curves 3 and 4 refer to calculations by formulas (9) and (10), respectively.

$$\varphi_w = 0, \qquad \frac{\partial \varphi_w}{\partial \boldsymbol{n}} = 0. \tag{8}$$

At the initial time t_0, we specify the position of the boundaries, the rate of submergence, the velocity potential on the entire boundary of the fluid domain $\varphi = 0$, and the pressure in the cavern $p = p_0$.

Algorithm of Solution. We solve the Cauchy problem for system (2) and (4) by a step-by-step method. For this, we introduce a difference scheme of the first order in time. To solve problem (5)–(8), we use the BEM with quantization of the boundaries Γ_{sw} and Γ_{wa} [7].

In each ith time step, the algorithm of solution is as follows.

1. The volume of the cavern is obtained from the position of the boundaries at the times t_i and t_{i-1}, and the pressure in the cavern is then found from Eq. (1). At the time t_1, the initial conditions are taken into account.

2. The boundary-value problem (5)–(8) is solved. In this case, boundary conditions (6) and (7) are specified from the solution of the problem in the previous step t_{i-1} using the current (in the step t_i). As a result, we determine $v_{nm} = (\partial\varphi/\partial \boldsymbol{n})_w$ on the boundary Γ_{wa} and φ_w on the surface Γ_{sw}. The tangential velocities on the boundaries are obtained by the finite-difference method from the values of the velocity potential at the nodes. The position of the boundaries is thus completely determined.

3. From Eq. (2) we calculate the pressures at the nodes of the body surface Γ_{sw}. For this, we determine beforehand the values of $(\partial\varphi/\partial t)_{sw}$ at the nodes:

$$\Big(\frac{\partial \varphi}{\partial t}\Big)_{sw} = \Big(\frac{d\varphi}{dt}\Big)_{sw} - v_{sw}^2, \qquad \Big(\frac{d\varphi}{dt}\Big)_{sw} \approx \frac{\varphi_{sw}(t_i) - \varphi_{sw}(t_{i-1})}{\Delta t}.$$

4. The velocity potential φ_w on the boundary Γ_{wa} is calculated:

$$\varphi_w(t_i) = \Big(\frac{d\varphi}{dt}\Big)_w \Delta t + \varphi_w(t_{i-1}).$$

In this case, using (2) and (3), we have

$$\Big(\frac{d\varphi}{dt}\Big)_{wa} = \Big(\frac{\partial \varphi}{\partial t}\Big)_{wa} + v_{wa}^2 = \frac{v_{wa}^2}{2} - g z_w - \frac{p_a - p_0}{\rho_w}.$$

5. From Eq. (4) we determine the current acceleration of the body $\dot v_s$ and, then, the velocity: $v_s(t_i) = v_s(t_{i-1}) + \dot v_s(t_i)\Delta t$.

6. The new position of the boundaries is calculated. The calculation grid is rearranged. The boundary parameters at the nodes of the new grid are found by interpolation.

Calculation Results. The algorithm for solving the problem of impact submergence ignoring the air layer was tested for a number of models [7]. Figure 2 shows the submergence force versus time for a rectilinear wedge with a deadrise angle of 10° moving with a velocity of 15 m/sec. The calculation results were compared to the solution

using the finite element method [3] taking into account the fluid compressibility and to results of calculations by the Wagner formulas

$$F = \rho\pi v_s^2 z_0(\pi/(2\tan\beta))^2, \tag{9}$$

$$F = \rho\pi v_s^2 z_0(\pi/(2\beta) - 1)^2, \tag{10}$$

where z_0 is the submergence of the vertex of the wedge and β is the deadrise angle.

To formulate recommendations on designing the bottom shape at the head of vessels prone to slamming, we performed numerous computational experiments on submergence of corrugated bottoms, in which we varied the shape and dimensions of corrugations and the initial velocity and mass of the vessel. Some results are presented in Figs. 3–5.

Let us consider the plane problem of the fall of a body on water for a body of length L having a bottom with "triangular corrugations" (see Fig. 1) with a width of 10 m and a relative mass of $Ma/(BL) = 10$ tons/m. The dimensions of this model correspond approximately to the dimensions of a concave ship bottom.

Figure 3 gives time dependences of the impact force and maximum pressure for various conditions. The solution of the problem is in agreement with Wagner's theory if the body moves at constant speed. In addition, we ignore the effect of the air layer, the weight of the fluid, and the mutual influence of neighboring corrugations, which, becoming more significant during submergence, leads to an increase in load. During free fall of the body, the impact load increases only in the first phase of impact, after which there is deceleration of the motion, and the load decreases.

The effect of the air layer can be different. At a small initial velocity ($v_{s0} \approx 1$ m/sec), the impact force increases as a result of intense air compression immediately after the bottom edges touch the water (Fig. 3). After that, because of deceleration of submergence, the load decreases rapidly and takes a constant value.

At a relatively high initial velocity (5–10 m/sec), the process of submergence changes qualitatively. In the first phase of impact, the load is determined primarily by hydrodynamic pressure. The effect of air is significant in the middle and at the end of impact.

Figure 4 shows the surface boundaries and pressure profiles at various times for a model with corrugations 2.1 m wide and an initial velocity of 5 m/sec. In this case, from the time 0.006 sec, the pressure in the air layer becomes higher than the average hydrodynamic pressure. Within 0.009 sec after the moment of initial contact, the impact force reaches the largest value (Fig. 5).

Test calculations for models with various layouts of boundaries showed that rapid convergence of results is achieved even with simple boundary elements (with constant approximation lengthwise). Usually, if the boundary contour is fairly smooth, 15–25 boundary elements on the wetted part of the vessel and 20–30 boundary elements on the water surface in the cavern ensure adequate accuracy of results (error of spatial quantization not higher than 1–5%).

The error of sampling depends on the ratio between the space and time steps, the impact parameters, and the assumptions used. For example, calculation results for models taking into account air and the mutual effect of corrugations are more sensitive to change in sampling.

Conclusions. The effects of the dimensions, corrugation shape, and impact velocity on the impact force are determined from results of numerical experiments (some of which are presented in Fig. 5). The effect of the corrugation shape on the pressure profile is also studied. The main conclusions from the investigation are as follows.

The developed numerical model and calculation procedure can be used for effective solution of problems of the impact exerted on fluids by bodies with carinate or corrugated bottoms.

The validity of the model is confirmed by results of test calculations and analysis of the effect of various assumptions on parameters of the submergence process (see Figs. 2 and 3).

From the calculation results it follows that the magnitude of the impact force is most strongly affected by the initial impact velocity, the height of corrugation, and the mass of the falling body. The effect of the corrugation shape is less significant (see Fig. 5).

Under conditions typical of slamming of marine vessels, the maximum of the impact force for a corrugated bottom is mainly due to the pressure in the air cavern (see Figs. 3a and 5). The impact force decreases with increase in the volume of air caverns due to appropriate choice of the corrugation shape.

The pressure peak on the wetted surface is pronounced and moves during submergence. As a result of deceleration of motion, the pressure in the valley of a corrugation can decrease to values at which cavitation is possible (see Fig. 4).

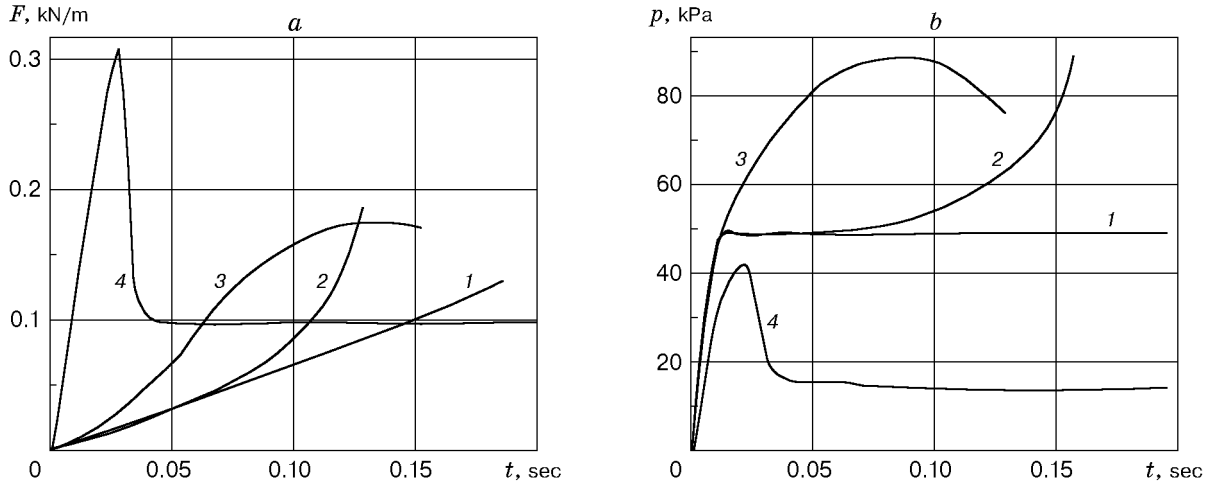

Fig. 3. Impact force (a) and maximum pressure (b) versus time for submergence of a bottom with triangular corrugations [$h/a = 0.05$, $a = 10$ m, $Ma/(BL) = 10$ tons/m, and $v_{s0} = 1$ m/sec): 1) without air, $v = \text{const}$, and single wedge; 2) without air and $v = \text{const}$; 3) without air; 4) with air.

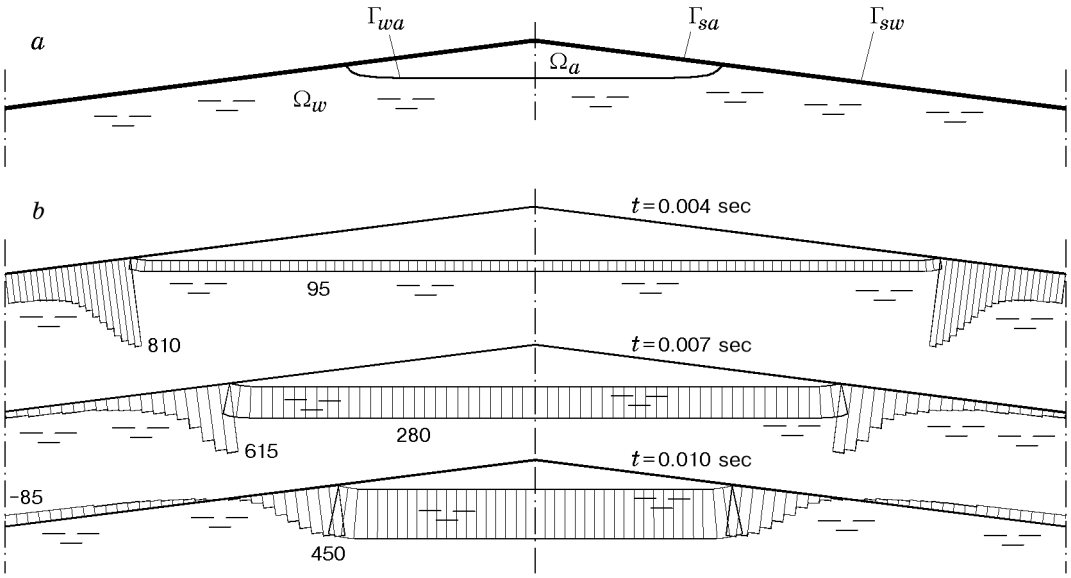

Fig. 4. Submergence of a bottom with triangular corrugations [$a = 2.1$ m, $h/a = 0.05$, $v_{s0} = 5$ m/sec, and $Ma/(BL) = 3$ tons/m): (a) surface boundaries (Ω_a is the region of the cavern, Ω_w is the fluid region, Γ_{wa} is the free boundary of the fluid in the cavern, Γ_{sa} is the interface between the body and the cavern, and Γ_{sw} is the interface between the body and the fluid); (b) pressure profiles for various times.

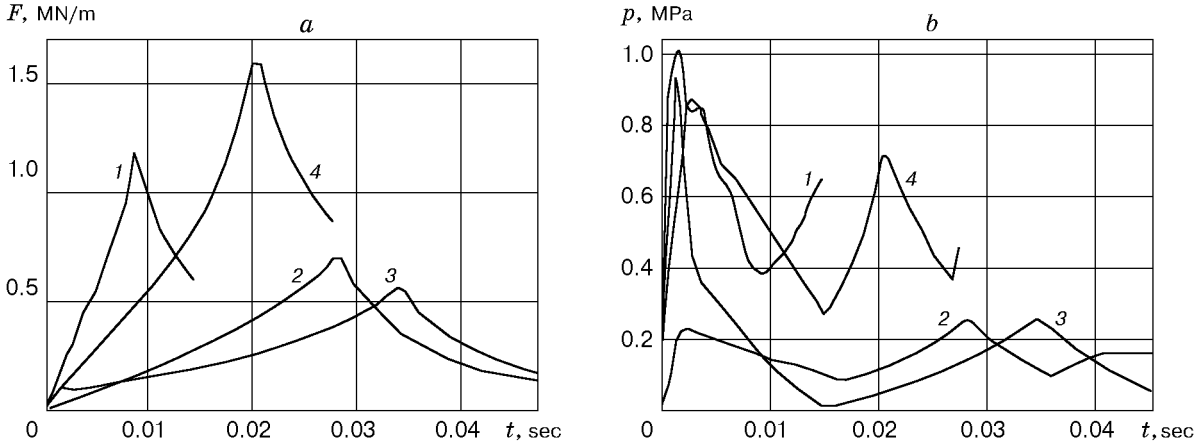

Fig. 5. Impact force (a) and maximum pressure (b) versus time for impact of a corrugated bottom ($a = 2.1$ m and $Ma/(BL) = 3$ tons/m): curves 1 refer to triangular corrugations for $h/a = 0.05$ and $v_{s0} = 5$ m/sec, curves 2 refer to triangular corrugations for $h/a = 0.2$ and $v_{s0} = 5$ m/sec, curves 3 refer to wavy corrugations for $h/a = 0.2$ and $v_{s0} = 5$ m/sec, and curves 4 refer to triangular corrugations for $h/a = 0.2$ and $v_{s0} = 10$ m/sec.

The impact force acting on a bottom with wavy corrugations is smaller than that acting on a surface with triangular corrugations (see Fig. 5). For wavy corrugations, the pressure concentrates near the vertices (as a result of hydrodynamic impact) and in the valleys (because of air pressure). For triangular corrugations, the peak pressure moves along the contour during submergence (see Figs. 4 and 5).

The results obtained can be used in designing new shapes of vessel bottoms taking into account the load during impact on water. The optimal shape and dimension of corrugations can be determined in numerical experiments using the proposed procedure, according to parameters and operation conditions of designed vessels.

REFERENCES

1. S.-W. Chau, C.-Y. Lu, and S.-K. Chou, "Numerical simulation of nonlinear slamming process for a high-speed planning vessel," in: *Proc. of the 14th Asian Technical Exchange and Advisory Meeting on Marine Structures*, TEAM-2000 (Vladivostok, September 18–21, 2000), Far East. State Tech. Univ., Vladivostok (2000), pp. 224–232.
2. V. D. Grigor'ev anmd V. A. Postnov, "Numerical algorithm of solution for a nonstationary problem of hydroelasticity in the presence of a free fluid surface," in: *Dynamics and Strength of Ship Designs*, Leningrad Shipbuilding Institute (1986), pp. 40–62.
3. N. F. Ershov and G. G. Shakhverdi, *Finite-Element Method in Problems of Hydrodynamics and Hydroelasticity* [in Russian], Sudostroenie, Leningrad (1984).
4. G. G. Shakhverdi, *Impact Interaction of Ships with a Fluid* [in Russian], Sudostroenie, St. Petersburg (1993).
5. V. A. Korobitsyn, "Numerical simulation of axisymmetric potential flows of an incompressible fluid," *Mat. Model.*, **3**, No. 10, 42–49 (1991).
6. K. Brebbia, J. Telles, and L. Wrobel, *Boundary Element Techniques*, Springer, Heidelberg (1984).
7. S. D. Chizhiumov, *Numerical Models in Problems of Ship Dynamics* [in Russian], Izd. Dal'nevost. Univ., Vladivostok (1999).